Supplementary Information (SI) for Journal of Materials Chemistry C.

Supporting Information for:

Enhanced thermoelectric performance of SnTe thin films by magnetron co-sputtering with optimized carrier concentration and microstructure

Hong-yue Du[1], Ye-chong Zhang[1], Wei Li[2], Yong Lu[1, *], and Jicai Zhang[1, 3, †]

[1]College of Mathematics and Physics, Beijing University of Chemical Technology, Beijing 100029, China
[2]School of Electronic Information Engineering, Lanzhou Institute of Technology, Lanzhou 730050, China
[3]State Key Laboratory of Chemical Resource Engineering, Beijing University of Chemical Technology, Beijing 100029, China
[*] Corresponding author: luy@mail.buct.edu.cn
† Corresponding author: jczhang@mail.buct.edu.cn

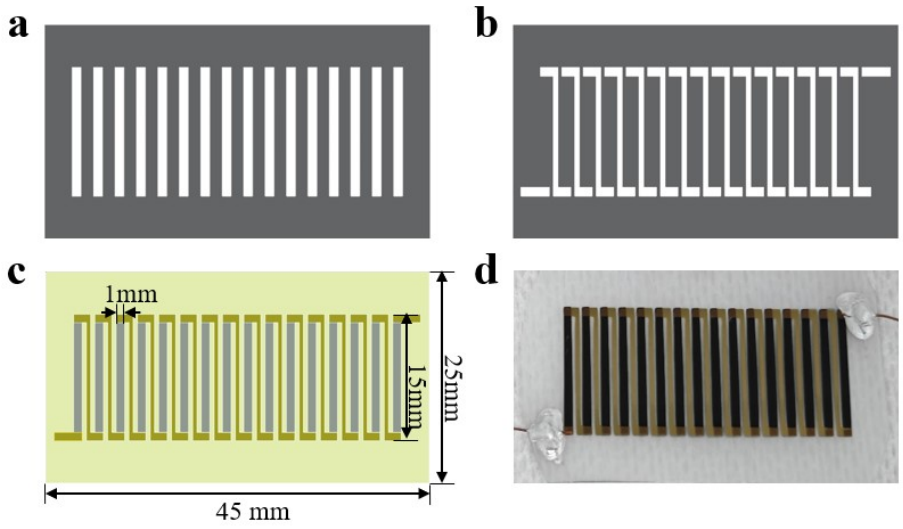

Figure. S1 Stainless steel mask used for (a) sputtering of SnTe films and (b) sputtering of gold electrodes; (c) Specification drawing and (d) physical drawing of thin-film thermoelectric generator.

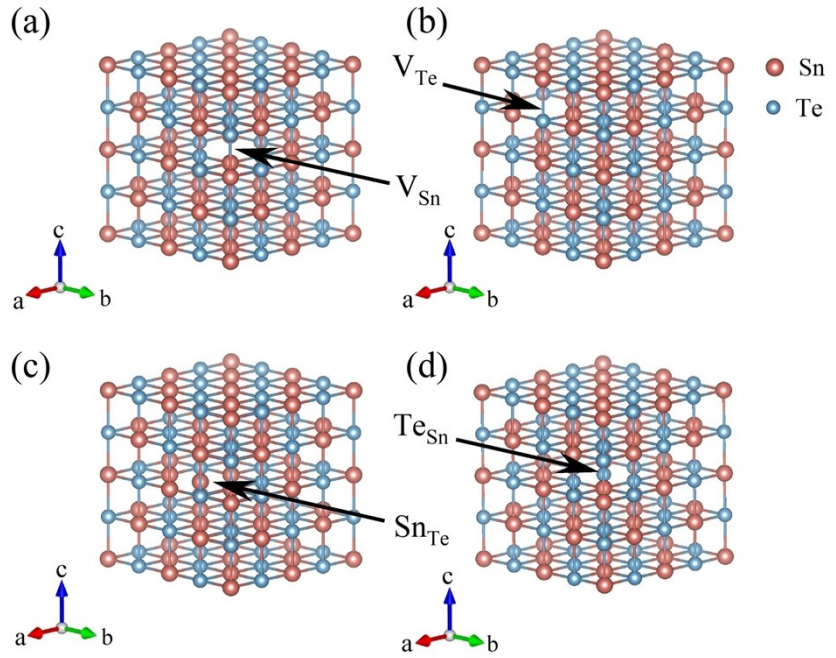

Figure S2. Computational supercell structures for vacancy and antisite defects in SnTe. (a) Sn vacancy (V_{Sn}). (b) Te vacancy (V_{Te}). (c) Sn antisite on Te sublattice (Sn_{Te}). (d) Te antisite on Sn sublattice (Te_{Sn}). Sn and Te atoms are represented by red and blue spheres respectively. The vacant sites are indicated by arrows.

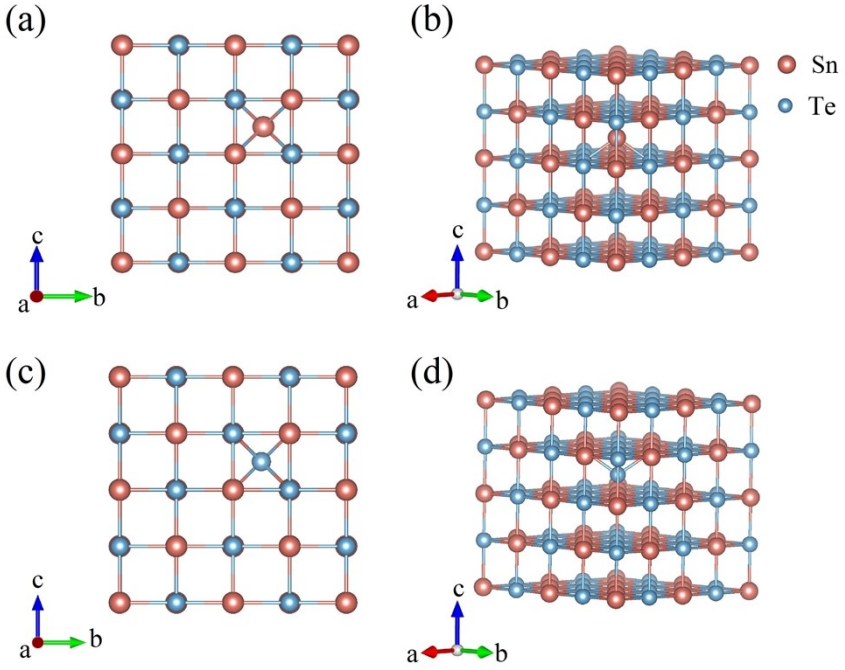

Figure S3. Computational supercell structures for interstitial defects in SnTe. (a), (b) Sn interstitial (Sn_i). (c), (d) Te interstitial (Te_i). Sn and Te atoms are represented by red and blue spheres respectively.

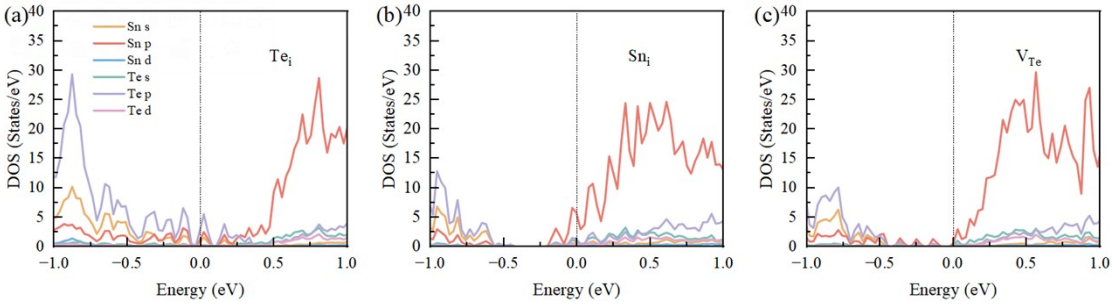

Figure S4. The calculated electronic density of states (DOS) for (a) Te interstitial Te_i, (b) Sn interstitial Sn_i, (c) Te vacancy V_{Te}.

Table S1. Experimental parameters of SnTe single-target sputtering (SnTe-ST) and SnTe-Te co-sputtering (SnTe-CT):

(a) The sputtering power of the SnTe target is variable. (In order to exclude the influence of film thickness on performance, experiments with different sputtering powers were carried out with the same thickness (all about 450 nm)).

SnTe(W)	Te(W)	T(℃)	Pressure(Pa)	Time(s)	P_{max}(nW)
20	0	Room temperature	2	3171	0.003
40	0	Room temperature	2	2400	0.087
60	0	Room temperature	2	1900	0.151
80	0	Room temperature	2	740	0.194
100	0	Room temperature	2	560	0.030

(b) The sputtering power of the Te target is variable

SnTe(W)	Te(W)	T(℃)	Pressure(Pa)	Time(s)	P_{max}(nW)
80	0	Room temperature	2	740	0.194
80	30	Room temperature	2	740	1.38
80	40	Room temperature	2	740	1.40
80	50	Room temperature	2	740	1.74
80	60	Room temperature	2	740	1.67

(c) The substrate temperature is variable

SnTe(W)	Te(W)	T(℃)	Pressure(Pa)	Time(s)	P_{max}(nW)
80	50	Room temperature	2	740	1.74
80	50	150	2	740	2.16
80	50	200	2	740	1.77
80	50	250	2	740	2.54
80	50	300	2	740	1.83

(d) The operating pressure is a variable

SnTe(W)	Te(W)	T(℃)	Pressure(Pa)	Time(s)	Pmax(nW)
80	50	250	1.5	740	0.98
80	50	250	2	740	2.54
80	50	250	2.5	740	1.692
80	50	250	3	740	1.637

(e) The best experimental parameters of the two films in this work (thickness is about 2um)

	SnTe(W)	Te(W)	T(℃)	Pressure(Pa)	Time(s)	Pmax(nW)
SnTe-ST	80	0	250	2	5000	7.83
SnTe-CT	80	50	250	2	5000	9.86

Table S2. Atomic compositions and numbers of atoms in the supercells used for the defect formation energy calculations of various defect types in SnTe.

	Sn atoms	Te atoms	Total
Perfect	32	32	64
V_{Sn}	31	32	63
V_{Te}	32	31	63
Sn_i	33	32	65
Te_i	32	33	65
Sn_{Te}	33	31	64
Te_{Sn}	31	33	64

Table S3. Detailed parameters and energy values used in the defect formation energy calculations, including the chemical potentials and total energies of the pristine and defective supercells under Sn-rich and Te-rich conditions:

(a) The parameters under Sn-rich growth conditions

	Sn-rich					
	V_{Sn}	V_{Te}	Sn_i	Te_i	Sn_{Te}	Te_{Sn}
E_{perf} (eV)	-242.05	-242.05	-242.05	-242.05	-242.05	-242.05
E_{def} (eV)	-237.33	-236.83	-243.89	-242.24	-241.29	-240.06
μ_{Sn} (eV)	-3.78	-3.78	-3.78	-3.78	-3.78	-3.78
μ_{Te} (eV)	-3.77	-3.77	-3.77	-3.77	-3.77	-3.77
E_f (eV)	0.93	1.43	1.94	3.58	0.76	1.97

(b) The parameters under Te-rich growth conditions

	Te-rich					
	V_{Sn}	V_{Te}	Sn_i	Te_i	Sn_{Te}	Te_{Sn}
E_{perf} (eV)	-242.05	-242.05	-242.05	-242.05	-242.05	-242.05
E_{def} (eV)	-237.33	-236.83	-243.89	-242.24	-241.29	-240.06
μ_{Sn} (eV)	-4.42	-4.42	-4.42	-4.421	-4.42	-4.42
μ_{Te} (eV)	-3.14	-3.14	-3.14	-3.14	-3.14	-3.14
E_f (eV)	0.29	0.79	2.58	2.94	2.03	0.70

Table S4. Energy values of the Fermi level, valence band maximum (VBM), and conduction band minimum (CBM) for various defect configurations.

	Fermi level (eV)	VBM (eV)	CBM (eV)
V_{Sn}	5.856	6.274	6.499
V_{Te}	6.530	6.108	6.474
Sn_i	6.534	6.137	6.305
Te_i	6.511	6.476	6.616
Sn_{Te}	6.183	6.458	6.598
Te_{Sn}	6.364	6.275	6.556
perfect	6.317	6.316	6.520

Table S5. The electronic thermal conductivity (κ_e) of the SnTe-CT and SnTe-ST samples at different temperatures obtained based on the measured electrical conductivity and Wiedemann–Franz relation.

	κ_e (W/mK)	
T(K)	SnTe-CT	SnTe-ST
300	3.33	2.72
350	3.35	2.86
400	3.51	3.06
450	3.57	3.22
500	3.65	3.36